Models for Slow Anisotropic Rotational Diffusion in Saturation Transfer Electron Paramagnetic Resonance at 9 and 35 GHz†

Michael E. Johnson,* Lana Lee, and Leslie W.-M. Fung*

ABSTRACT: Model systems of cholestane and 5-doxylstearic acid analogue spin probes in lipid bilayer dispersions of dipalmitoylphosphatidylcholine and cholesterol (9:1 w/w) are used to analyze saturation transfer electron paramagnetic resonance spectral behavior for slow rotational diffusion in an anisotropic medium. Measurements are made at both 9 and 35 GHz to provide enhanced spectral resolution for different types of motion. Parameter correlation plots of spectral parameters from different regions of the saturation transfer spectra appear to be potentially useful in characterizing different types of motion. Anisotropic rotational diffusion about a symmetry axis coincident with the nitroxide *y* principal axis is clearly distinguishable from isotropic rotational diffusion and may be distinguishable from rotational diffusion about the nitroxide *z* principal axis. Approximate anisotropic rotational diffusion about a symmetry axis coincident with the nitroxide *z* principal axis is distinguishable from isotropic rotational diffusion under some, but not all, conditions.

The application of spin-label rapid passage saturation transfer electron paramagnetic resonance (ST-EPR)[1] methods to the study of various membrane systems has shown a substantial increase over the last few years. Recent applications include the use of several spin probes to study motional behavior within the hydrocarbon region of model (Delmelle et al., 1980; Marsh, 1980; Marsh & Watts, 1980; Watts & Marsh, 1981) and erythrocyte (Swift et al., 1980; Fung, 1981) membranes, studies of rhodopsin in the visual receptor membrane (Kusumi et al., 1978, 1980; Baroin et al., 1979; Favre et al., 1979; Davoust et al., 1980), studies of the sarcoplasmic reticular ATPase (Kirino et al., 1978; Hidalgo et al., 1978; Thomas & Hidalgo, 1978), studies of the spectrin–membrane interaction in erythrocyte membranes (Fung et al., 1979; Lemaigre-Dubreuil et al., 1980; Fung, 1981), and studies of reconstituted cytochrome *c* oxidase (Swanson et al., 1980). Several of these and other applications are discussed in recent reviews (Hyde, 1978; Hyde & Dalton, 1979; Hyde & Thomas, 1980).

For many of these applications the ST-EPR spectral behavior suggests the existence of anisotropic motion, but analysis of such motion has been quite limited due to the lack of a detailed understanding of the effects of anisotropic motion upon ST-EPR spectral behavior. Anisotropic rotational diffusion can result from two different physical mechanisms: (a) a highly asymmetric molecule undergoing rotational diffusion in an isotropic medium and (b) a molecule (of arbitrary shape) undergoing rotational diffusion in an anisotropic medium which exhibits an orientational restoring potential. Each of these major diffusional mechanisms can also be further subdivided into diffusional processes depending on the relative sizes of solute and solvent molecules. These subdivisions include Brownian reorientation of a large molecule in a low molecular weight solvent, strong jump reorientation of a small molecule in a solvent of comparable or higher molecular weight, and free diffusion in which both Brownian and jump reorientation processes occur. Under most circumstances the two mechanisms produce different motional and spectral behaviors, with the detailed spectral behavior also depending on the precise diffusional process which is occurring. The second case, rotational diffusion in an anisotropic medium, is of most relevance to membrane problems and to a number of other biomolecular assembly problems and is the case considered in this work.

The problem of anisotropic motion in ST-EPR has been approached experimentally through the use of spin probe–thiourea adduct (Gaffney, 1979) and oriented lipid bilayer (Delmelle et al., 1980) model systems. These initial studies have shown that anisotropic motion produces substantial changes in the ST-EPR spectral display, particularly for the case where the diffusional and nitroxide magnetic symmetry axes are perpendicular to each other. Extensive theoretical calculations of ST-EPR spectral behavior have also been reported for the two cases where the diffusion tensor is either coincident with or orthogonal to the nitroxide magnetic tensor (Robinson & Dalton, 1980), but the calculations were for the out-of-phase dispersion (U_1') display, while most experimental studies have utilized the out-of-phase second harmonic absorption (V_2') display due to its simpler instrumental requirements and higher signal-to-noise ratios. Increasing the observational frequency from 9 (X band) to 35 GHz (Q band) to increase *g* anisotropy and spread out the spin states (Johnson & Hyde, 1981) and substituting the ^{15}N isotope for the naturally occurring ^{14}N in the spin-label nitroxide to decrease the number of spin states from three to two (Beth et al., 1981; Gaffney et al., 1981; Johnson et al., 1982) have also recently been shown to increase ST-EPR spectral resolution. These seem likely to become rather powerful approaches in future studies but have thus far been utilized only for isotropic model systems. Thus guidelines for characterizing anisotropic motion in the ST-EPR time domain are still quite limited.

As an approach to developing more detailed guidelines for characterizing anisotropic motion in the ST-EPR time domain,

† From the Department of Medicinal Chemistry, University of Illinois at the Medical Center, Chicago, Illinois 60680 (M.E.J.), and the Department of Chemistry, Wayne State University, Detroit, Michigan 48202 (L.L. and L.W.-M.F.). *Received August 7, 1981; revised manuscript received March 19, 1982.* This work was supported in part by grants from the Chicago Heart Association, the Michigan Heart Association, and the National Institutes of Health (HL-23697, HL-16008, and HL-22432). Facilities of the National Biomedical ESR Center are supported in part by a grant from the National Institutes of Health Division of Research Resources (RR-01008). M.E.J. is an Established Investigator of the American Heart Association. L.W.-M.F. is a National Institutes of Health Research Career Development Awardee (K04 HL-00860).

[1] Abbreviations: EPR, electron paramagnetic resonance; ST-EPR, saturation transfer EPR; DPPC, dipalmitoylphosphatidylcholine; 5-SASL, 5-(4,4-dimethyloxazolidinyl-*N*-oxy)stearic acid; CSL, 4′,4′-dimethylspiro[5α-cholestane-3,2′-oxazolidin]-3′-yloxy; Mal-6, 4-maleimido-2,2,6,6-tetramethylpiperidin-1-yloxy; Hb, hemoglobin; TPX, methylpentene polymer.

0006-2960/82/0421-4459$01.25/0

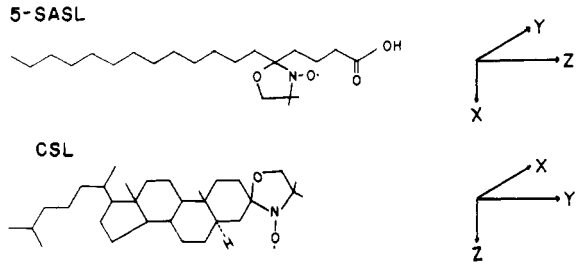

FIGURE 1: Orientation of nitroxide principal magnetic axes with respect to molecular structures of the 5-SASL and CSL spin probes used here. Rotational diffusion within the lipid bilayers occurs primarily about the long molecular axes of the spin probes.

we report here the X-band and Q-band ST-EPR spectral behavior of two model systems exhibiting axial rotational diffusion: (1) a DPPC–cholesterol dispersion with an incorporated stearic acid analogue spin probe in which the nitroxide principal z axis is approximately coincident with the diffusional symmetry axis (Griffith & Jost, 1976; Marsh, 1980) and (2) a DPPC–cholesterol dispersion with an incorporated cholestane analogue spin probe in which the nitroxide principal y axis is approximately coincident with the diffusional symmetry axis (Marsh, 1980; Polnaszek et al., 1981). Rotational diffusion of these spin probes within the lipid bilayer occurs primarily about the long molecular axes, shown in Figure 1. Oriented bilayer studies indicate that the cholestane analogue spin probe is highly oriented within DPPC–cholesterol bilayer systems, providing a very good model for y-axial diffusion, while the stearic acid probe is somewhat less ordered due to motional effects, resulting in a more approximate model for z-axial diffusion (Delmelle et al., 1980). At 9 GHz, we find that the V_2' ST-EPR spectral behavior exhibits qualitative similarities between the two systems. However, the quantitative behavior of the L''/L, C'/C, and H''/H spectral parameters defined by Thomas et al. (1976) differs between the two systems and, for both systems, differs significantly from that observed for isotropic rotational diffusion. Spectral parameter correlation diagrams of L''/L and H''/H vs. C'/C appear potentially useful as diagnostic indicators of axial anisotropic rotational motion. At 35 GHz, the spectral effects of anisotropic rotational diffusion are substantially greater than at 9 GHz, and the two types of axial motion can be distinguished somewhat more readily from each other, and from isotropic rotational motion. Parameter correlation plots for some of the 35-GHz spectral parameters defined by Johnson & Hyde (1981) also appear potentially useful as diagnostic indicators of anisotropic rotational diffusion.

Materials and Methods

Multilamellar lipid–cholesterol dispersions were prepared following procedures similar to those of Lentz et al. (1980); details are as follows. Commercial grade DL-DPPC and cholesterol (Sigma) were used without further purification. The 5-SASL and CSL spin probes (Syva Research Chemicals) were stored in reagent-grade chloroform. Mixtures of DPPC and cholesterol were prepared from 9 parts DPPC and 1 part cholesterol (by weight). At this cholesterol concentration (~20 mol %), the bilayers appear to be in an essentially homogeneous phase with DPPC and cholesterol uniformly distributed in an approximate 4:1 molar ratio (Recktenwald & McConnell, 1981). The spin probe (either 5-SASL or CSL) was added to this mixture at a DPPC to spin probe weight ratio of 400:1. Excess chloroform was added to dissolve all components. The chloroform was then evaporated to dryness under nitrogen to give a thin film of lipid in the container. Final removal of residual chloroform was done overnight under high vacuum. About 0.7 mL of 0.05 M sodium phosphate buffer at pH 6.7 was then added to 100 mg of the dried lipid–cholesterol mixture. The lipid dispersion was prepared by warming the sample to 50 °C, incubating for 1–2 min, and vortexing vigorously for about 30 s. This cycle of heating and vortexing was repeated continuously for about 10–15 min until all lipid was homogeneously dispersed in solution. Ethylene glycol was added to the dispersion to give a final concentration of 30% by volume of ethylene glycol. Previous work has shown that ethylene glycol at this concentration lowers the water freezing point but does not alter the lipid phase transition (Johnson et al., 1973). Samples were then centrifuged with an SS-34 rotor at 10000 rpm for 30 min to pack the lipid samples. Most of the supernatant was removed, and the samples were purged with nitrogen and stored under nitrogen atmosphere at 4 °C until used for EPR experiments. For 9-GHz EPR measurements, samples were introduced into a specially constructed gas-permeable TPX capillary with a 1-mm i.d. [See Popp & Hyde (1981) for details on TPX properties.] The samples were introduced to the EPR cavity, and the cavity was flushed with nitrogen until the C'/C ratio reached a constant value, indicating that dissolved oxygen had been removed from the sample (Popp & Hyde, 1981). For 35-GHz measurements, the samples and EPR tubes (5-μL Corning borosilicate glass disposable pipet capillaries) were both purged with nitrogen for about 30 min prior to EPR sample preparation. EPR measurements were performed immediately after sample preparation. X-band EPR measurements were performed on a Varian E109E spectrometer with second harmonic absorption (V_2') and first harmonic dispersion (U_1') capabilties. Q-band EPR measurements were performed on a modified Varian E-9 spectrometer with V_2' and U_1' capabilities. Standard procedures for X-band (Fung, 1981) and Q-band (Johnson & Hyde, 1981) EPR operation were followed. At X band the microwave power was set to provide an intensity at the sample equivalent to the 63-mW level used by Thomas et al. (1976). At Q band, settings equivalent to those of Johnson & Hyde (1981) were used. Nitrogen gas was used for temperature control in both X- and Q-band operation.

Results

Measurements at 9 GHz. The lower portion of Figure 2 shows the spectral behavior of the 9-GHz V_2' display for the two DPPC–cholesterol model systems over the temperature range −30 to +30 °C. From −30 up to about 0 °C the spectral behavior is qualitatively quite similar for the two systems. Above 0 °C, however, there are moderate differences between the outer wings of the spectra for the two systems. For the DPPC–cholesterol dispersion with incorporated 5-SASL, the high-field turning point (H) is well resolved at all temperatures, while the high-field region for the CSL system essentially becomes a plateau with a poorly resolved turning point at temperatures above 0 °C. [See Johnson & Hyde (1981), Thomas et al. (1976), and Hyde & Dalton (1979) for discussions of the physical significance of the turning points.] Likewise, the L'' region for the CSL system appears to flatten out and move in toward the center of the spectrum as the temperature increases to +30 °C, while the same region remains fairly well resolved over the full temperature range for the 5-SASL system. Thus, for the faster motions corresponding to the higher temperatures, a simple examination of the V_2' spectra is probably adequate to distinguish between the two types of motion. However, for slower motions, as would probably be observed for such systems as membrane proteins, the two types of motion yield qualitatively similar

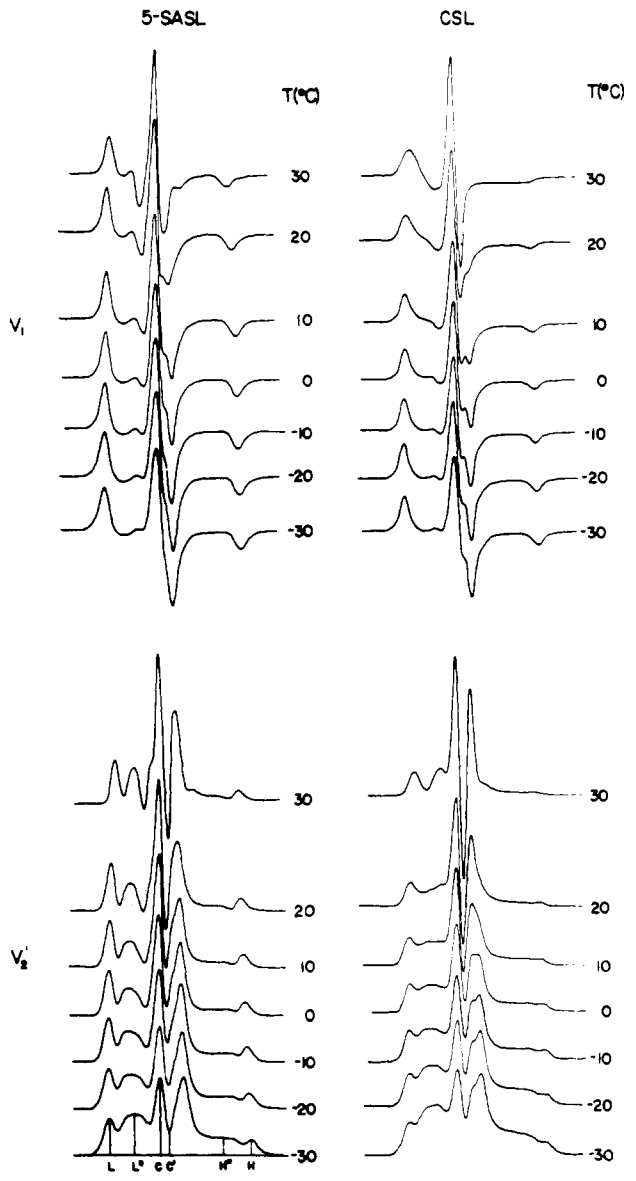

FIGURE 2: 9-GHz spectra of 5-SASL (left column) and CSL (right column) incorporated into water–ethylene glycol (70:30) dispersions of DPPC–cholesterol (90:10 w/w). Conventional in-phase first harmonic absorption (V_1) spectra are shown in the top portion of the figure. Second harmonic out-of-phase (V_2') ST-EPR spectra for the two systems are shown in the bottom portion of the figure. Concentrations of the 5-SASL and CSL spin probes are both approximately 0.5 mol %; no spin-exchange interactions were observed at this concentration for either probe. Both systems are thoroughly deoxygenated to eliminate oxygen–spin probe induced relaxation effects (Popp & Hyde, 1981). Spectra were obtained by lowering the sample temperature to −30 °C and then progressively raising the temperature for each new observation; the samples were allowed to equilibrate for about 30 min at each temperature before the spectrum was recorded.

spectral displays and require more detailed analysis, as described below.

The out-of-phase dispersion (U_1') display has been used extensively for calculations of the effects of anisotropic motion on ST-EPR spectra (Robinson & Dalton, 1980); thus U_1' spectra for the two model systems at several temperatures are also shown in Figure 3. These spectra show much less sensitivity to changes in motion than do the V_2' spectra of Figure 2, and differences between the spectral behaviors of the 5-SASL and CSL systems are substantially less obvious in the U_1' than in the V_2' display. Furthermore, while "*L*" and "*H*" ratios analogous to those defined by Thomas et al. (1976) for the V_2' display may also be defined for the U_1' display, there

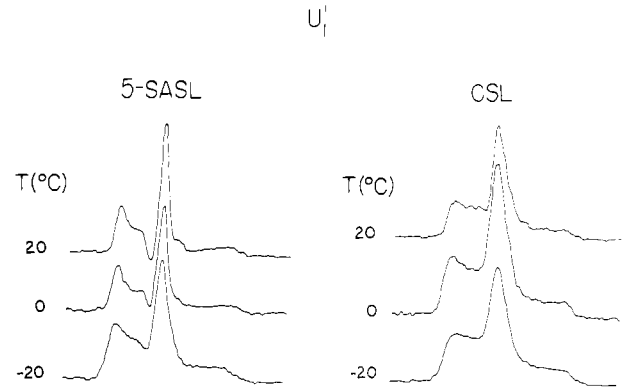

FIGURE 3: 9-GHz first harmonic out-of-phase dispersion (U_1') spectra of 5-SASL (left) and CSL (right) incorporated into aqueous dispersions of DPPC–cholesterol mixtures. Conditions are as noted for Figure 2. The spectra for both systems show relatively little change with temperature; thus only spectra for the three temperatures −20, 0, and +20 °C are shown.

is no comparable "*C*" ratio which may be readily defined for the U_1' spectra (Fung, 1981). Since the central region of the spectrum is primarily defined by the *x* and *y* nitroxide magnetic tensor elements, this lack of a readily definable *C* parameter results in the loss of much of the motional anisotropy information. From these considerations we are coming to believe that the U_1' display is of limited value except for special systems where detailed spectral simulations may be calculated.

Figure 4 compares the 9-GHz V_2' ST-EPR spectral parameters for *y*-axial motion (CSL in DPPC–cholesterol), approximate *z*-axial motion (5-SASL in DPPC–cholesterol), and isotropic motion (Mal-6-labeled Hb in water–glycerol solutions). [The isotropic data are taken from the published curves of Thomas et al. (1976); spectrometer settings in this work were set to yield calibration curves equivalent to those of Thomas et al. (1976).] From a comparison of the behavior of the CSL–DPPC–cholesterol system with that for isotropic motion, it is apparent that the minimum values of the L''/L and H''/H parameters for *y*-axial motion are much larger than the minima observed for isotropic motion. The L''/L ratio for the CSL system goes through a minimum of about 0.8 at about 15 °C, compared with a minimum value of about 0.1 for isotropic motion. The H''/H ratio for the CSL system plateaus at a minimum value of about 1.0 at about 0 °C and then increases again for temperatures above 20–25 °C. In contrast, for isotropic motion, the H''/H ratio decreases monotonically to zero as motion increases. The C'/C ratios for both the CSL system and the isotropic motion model exhibit qualitatively similar behavior, with a comparable range of values. The overall spectral behavior of the CSL–DPPC–cholesterol system observed here is quite similar to that reported by Gaffney (1979) for CSL–thiourea adducts in which the CSL spin probe exhibits rotational diffusion with *y*-axial symmetry within channels in the crystal adduct. Thus it would appear that the ST-EPR spectral behavior is primarily dependent on the type(s) of rotational motion occurring and is not particularly sensitive to the specific system used.[2]

[2] One of the referees has pointed out that the low-temperature limiting behaviors of the *L* and *H* spectral parameters do not appear to be equivalent for all of the systems shown in Figure 4. This appears to be largely due to differences in residual label motion between the different systems at the temperatures shown, and to differences in dipolar line broadening between different conditions, but is not an intrinsic difference between systems. If the temperature is reduced to the range −80 to about −100 °C, the V_2' spectra for all systems go asymptotically toward a broadened absorption envelope. This problem has been discussed to some extent in previous work (Johnson, 1978, 1979, 1981).

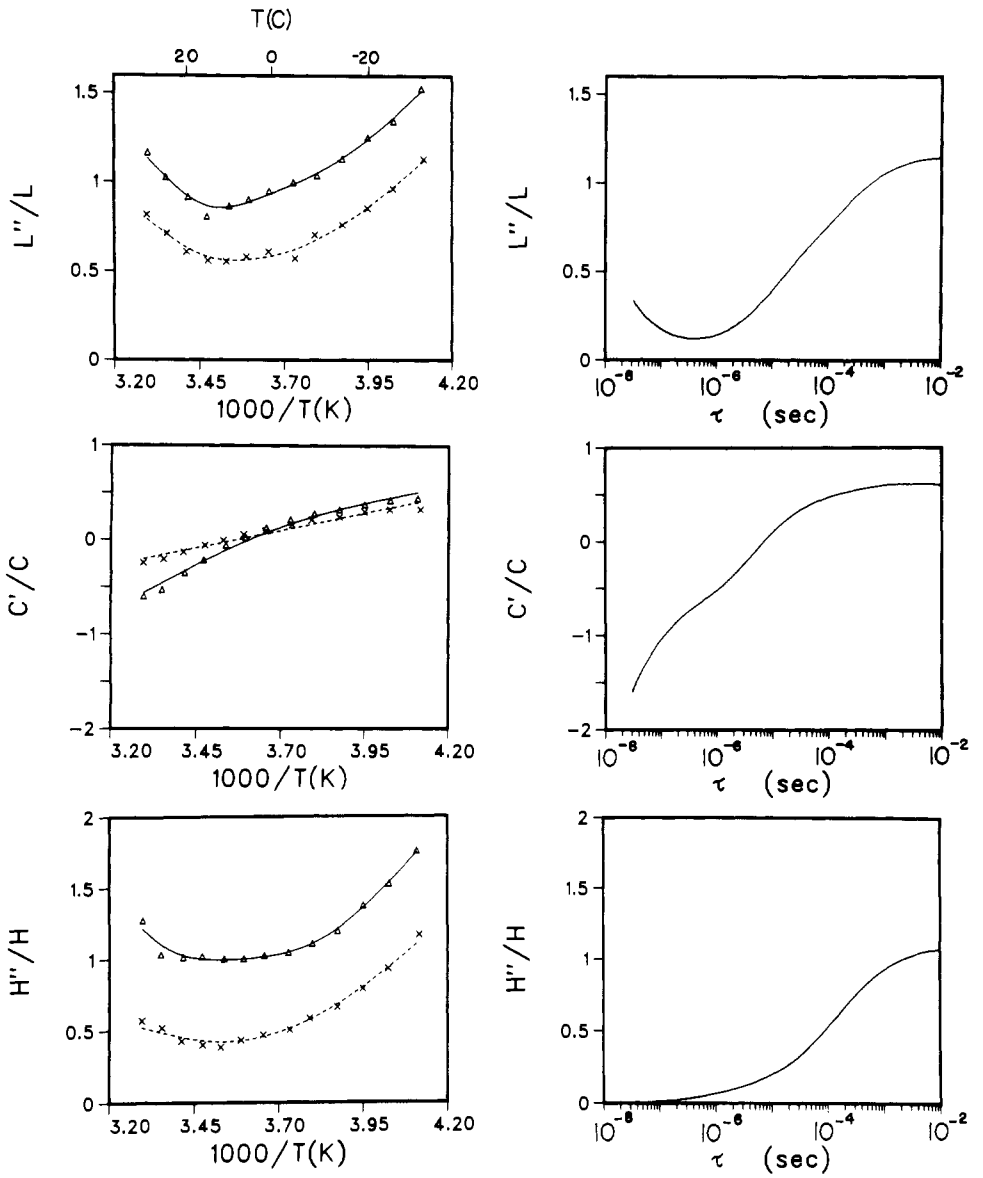

FIGURE 4: 9-GHz V_2' ST-EPR spectral data for the axial motions of the CSL spin probe in a DPPC–cholesterol dispersion [(Δ) left column] and the 5-SASL spin probe in a DPPC–cholesterol dispersion [(×) left column] are compared with the data for isotropic motion of Mal-6-labeled Hb in water–glycerol solutions of varying viscosity (smooth lines, right column). The isotropic motion data are taken from the published figures of Thomas et al. (1976); comparable data were obtained on the spectrometer used in this study for the same model system; thus we have simply used the data from the published curves. Data for the three commonly used L, C, and H spectral ratios are shown. Vertical scales of the axial and isotropic motion plots are made equivalent for each of the spectral ratios to facilitate comparisons of qualitative behavior. Data for the two axial motion systems are shown as a function of inverse absolute temperature; increasing values of the abscissa thus correspond to slower motional rates for both axial and isotropic motions.

For the 5-SASL–DPPC–cholesterol system, which undergoes approximate z-axis rotational diffusion, the L''/L and H''/H spectral parameters exhibit behaviors somewhat closer to those of the isotropic model, but there are still significant qualitative differences between the two systems. The L''/L ratio for the 5-SASL system goes through a minimum of about 0.55 at ~10 °C, compared with minima of about 0.8 and 0.1 for the CSL and isotropic model systems, respectively. Likewise, the H''/H ratio for the 5-SASL system goes through a broad minimum of about 0.4, compared with a minimum value of about 1.0 for the CSL system and a monotonic decrease to zero for the isotropic model. The C'/C ratio for the 5-SASL system again exhibits behavior qualitatively similar to that of both the CSL system and the isotropic motion model, but with a somewhat more limited range of values.

The spectral differences observed here for the three types of motion, y-axial, approximate z-axial, and isotropic, indicate that it should be feasible to distinguish between them in various experimental systems. However, simply comparing spectral ratios in plots similar to those of Figure 4 does not lead to any obvious resolution of the problem, since the ratios are all multivalued, varying with changes in motional rates. Thus a simple method for simultaneously comparing spectral behaviors in different regions of the spectrum is needed.

One solution to this problem is the use of parameter correlation plots in which one spectral parameter is plotted against another. The observation that the L''/L and H''/H ratios exhibit significant differences in behavior between the different types of motion but that the C'/C ratio exhibits similar behavior for all three types of motion studied suggests that L''/L and H''/H vs. C'/C may be particularly useful representations of the data. Plots of this form are shown in Figure 5. From these two plots, it can be seen that the three types of motion exhibit substantially differing spectral behaviors over nearly the complete motional range from fast motion up to almost complete immobilization. The H''/H vs. C'/C plot appears

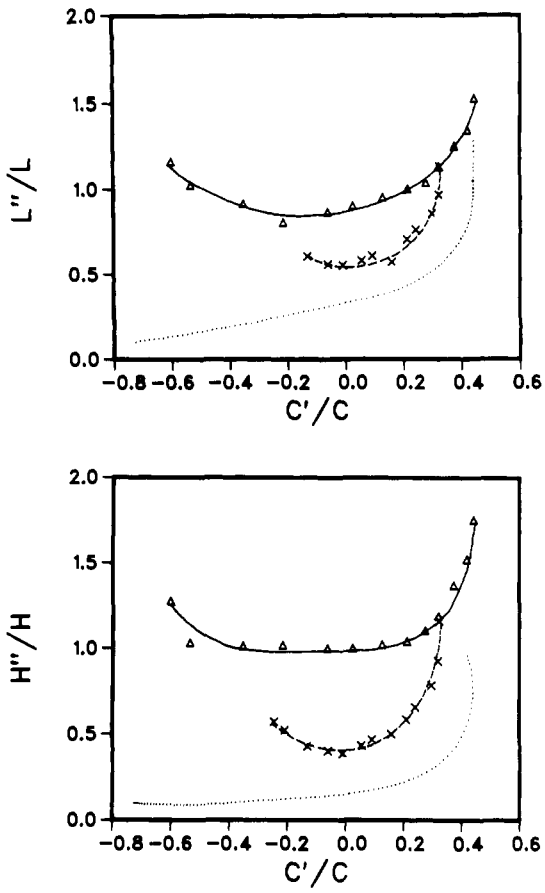

FIGURE 5: 9-GHz parameter correlation plots of L''/L vs. C'/C and H''/H vs. C'/C for the data of Figure 3. The spectral behaviors of CSL in DPPC–cholesterol (△) (y-axial motion) and 5-SASL in DPPC–cholesterol (×) (approximate z-axial motion) are compared with that of Mal-6-labeled Hb in water–glycerol solutions (···) (isotropic motion). Isotropic motion data are from the published curves of Thomas et al. (1976). High-temperature cutoffs of 30 °C were used for the two lipid systems to ensure that the spectral ratios were measured only under conditions where the "turning points" were nearly stationary (see Discussion). The range of isotropic data displayed was chosen to correspond to the spectral parameter ranges exhibited by the two axial motion models.

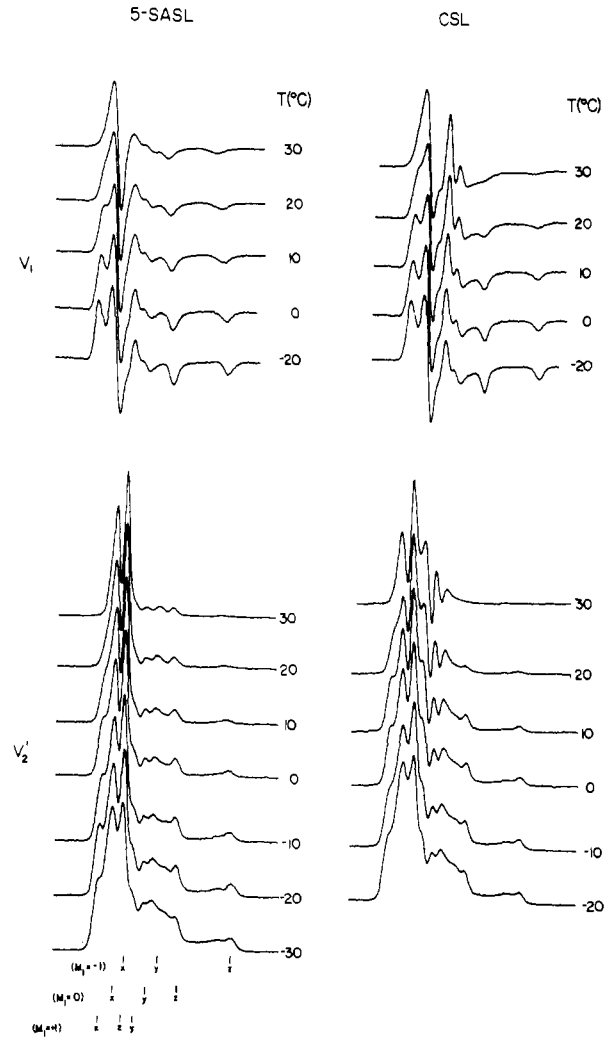

FIGURE 6: 35-GHz spectra of 5-SASL (left column) and CSL (right column) incorporated into DPPC–cholesterol dispersions. Sample conditions are as described in Figure 2. Conventional in-phase first harmonic absorption (V_1) spectra are shown in the top portion of the figure. V_2' spectra for the two systems are shown in the bottom portion of the figure. Approximate positions of the turning points for the three spin states are shown below the 5-SASL V_2' spectrum in the lower left corner.

to show the greater resolution between types of motion, but the L''/L parameter is experimentally much easier to measure than is H''/H.

The principal advantage of presenting the spectral data in the form of parameter correlation plots is that qualitative information about the motional behavior of an experimental system may be directly obtained by generating spectral ratio curves similar to those of Figure 5 (by varying temperature or medium viscosity, etc.) and by comparing with those from the axial motion and isotropic motion model systems. The choice of using the "L" or "H" parameter will depend on the particular system of interest.

Measurements at 35 GHz. The upper portion of Figure 6 shows the conventional V_1 spectra for 5-SASL and CSL incorporated into DPPC–cholesterol dispersions from +30 down to −20 °C. From +30 °C down to +10 °C, the two types of motion are distinguishable from each other simply from a comparison of the effects of motion on the outer spectral turning points. At this observational frequency the g anisotropy has moved the $x(+1)$ turning point to the downfield edge of the spectrum, while the $z(-1)$ turning point defines the high-field edge of the spectrum. At the high temperatures the $x(+1)$ turning point has undergone motional averaging with other regions of the spectrum for both the 5-SASL and CSL systems. However, the high-field $z(-1)$ turning point is undergoing much more motional averaging for the CSL system than for the 5-SASL system. Thus 35-GHz observation would lead directly to the conclusion that the CSL system is undergoing x–z averaging while the 5-SASL system is undergoing approximate x–y averaging. In contrast, at 9 GHz the V_1 spectra in the upper portion of Figure 2 indicate that the CSL system is producing much greater motional averaging of the z turning points than is the 5-SASL system but, without detailed analysis, indicate little about the mechanism for the differential effects.

Below about +10 °C the turning points are all essentially stationary, and the 35-GHz V_1 spectra yield little useful motional information (Figure 6). Under these conditions the V_2' spectra, shown in the portion of Figure 6, yield more useful information about motional behaviors. From a comparison of the V_2' spectra for these two systems, it appears that there are moderate differences in spectral behavior, particularly in the central region which is dominated by the y turning points for all three spin states. This suggests that the 35-GHz V_2' spectral ratios B'/B, C'/C, and D'/D evaluated by Johnson & Hyde (1981) might be most useful for comparing the be-

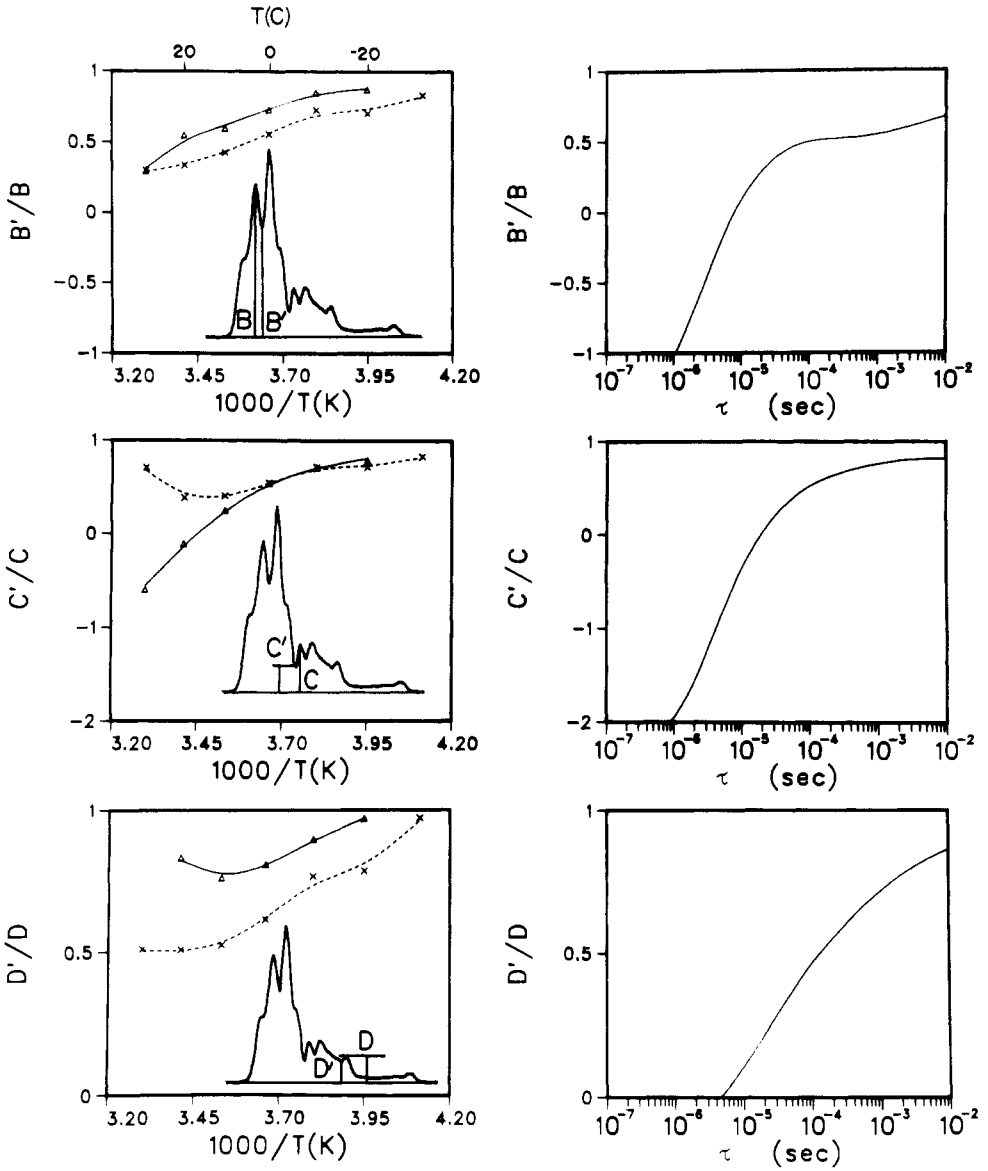

FIGURE 7: 35-GHz V_2' ST-EPR spectral data for the axial motions of the CSL spin probe in a DPPC–cholesterol dispersion [(Δ) left column] and the 5-SASL spin probe in a DPPC–cholesterol dispersion [(×) left column] are compared with the data for isotropic motion of Mal-6-labeled Hb in water–glycerol solutions of varying viscosity (solid curves, right column). The isotropic motion data are taken from the published curves of Johnson & Hyde (1981). Data for the three 35-GHz spectral ratios which appear most sensitive to differences between the two types of axial motion and isotropic motion are shown. Data for the two lipid systems are shown as a function of inverse absolute temperature; increasing values of the abscissa thus correspond to slower motional rates for all three types of motion. Data for the isotropic case has been restricted to roughly the range of values exhibited by the two axial motion systems. Vertical scales for each of the parameters are equivalent for the axial and isotropic motion plots to facilitate comparison.

havior of these model systems.

Figure 7 compares the behavior of these three 35-GHz V_2' ST-EPR spectral parameters for the two axial motion systems and for isotropic motion [isotropic motion data from the published curves of Johnson & Hyde (1981)]. For all three parameters the range of values exhibited by both axial motion systems is much more restricted than that exhibited by the isotropic model. The maximum parameter values in the limit of immobilization is about the same for all three systems, but the minimum values exhibited in the fast motion limit are much higher for both of the axial motion systems than for the isotropic motion model. The D'/D parameter also appears to provide some resolution of spectral behavior between the two axial motion systems over the temperature range studied here. For the CSL system it goes through a minimum of about 0.75 at about +10 °C, while for the 5-SASL system it goes to a minimum of about 0.5 for temperatures of +20 °C and above, and for isotropic motion it goes through zero to negative values for correlation times less (faster) than $\sim 10^{-5}$ s.

Parameter correlation plots of B'/B vs. C'/C and D'/D vs. C'/C are shown in Figure 8. (The C'/C parameter was chosen as the abscissa in these plots primarily due to its physical significance at 35 GHz being similar to that of the C'/C parameter at 9 GHz. However, the choise is arbitrary; the only requirement for the plots to be useful is that the parameters to be used vary differently from each other with different types of motion.) From these plots it appears that y-axial motion is readily distinguishable from both approximate z-axial and isotropic motions but that the appropriate z-axial motion is well distinguished from isotropic motion. From the locations of the turning points, D'/D should be particularly sensitive to loss of correlation between the nitroxide magnetic z-axis and the magnetic field, while the C'/C parameter should be primarily sensitive to x–y and x–z averaging (Johnson & Hyde, 1981). Thus the D'/D vs. C'/C correlation plot should be particularly useful for distinguishing between the types of axial

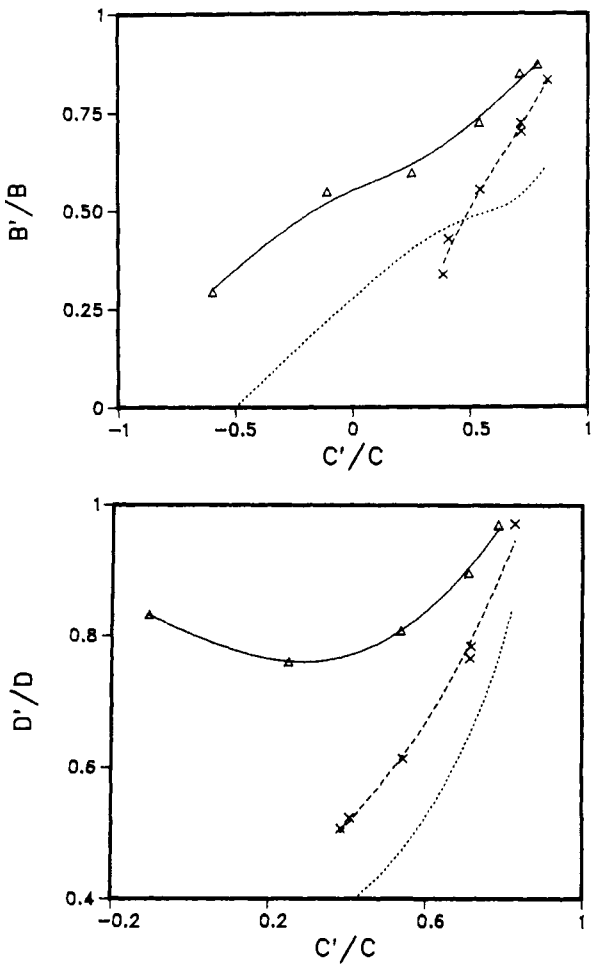

FIGURE 8: 35-GHz parameter correlation plots of C'/C vs. B'/B and D'/D vs. C'/C for the data of Figure 6. The spectral behaviors of CSL in DPPC–cholesterol [(△) y-axial motion] and 5-SASL in DPPC–cholesterol [(×) z-axial motion] are compared with that of Mal-6-labeled Hb in water–glycerol solutions [(···) isotrtropic motion]. Isotropic motion data are from the published curves of Johnson & Hyde (1981).

motion. The B'/B vs. C'/C correlation plot, while providing somewhat more limited resolution of the two axial motions, is more difficult to interpret since the B'/B parameter results from spin state–turning point overlap nearly as complex as that of the 9-GHz (X-band) C'/C parameter.

Discussion

The quantitative description of complex motions from ST-EPR observations in the slow motion time domain is a formidable problem which has been discussed in the literature (Gaffney, 1979; Delmelle et al., 1980; Marsh, 1980; Robinson & Dalton, 1980; Hyde & Dalton, 1979; Hyde & Thomas, 1980) but is still far from being solved. In this work we propose simple empirical methods to address the initial questions: Is the motion anisotropic? If the motion is anisotropic, can the diffusional symmetry be described with respect to the nitroxide magnetic frame of reference?

The results described above indicate that slow, anisotropic rotational diffusion about either the y or the z principal axis of the nitroxide leads to ST-EPR spectral behaviors which are characteristic for the types of motions occurring. At the same time several limitations in the generality of this work should be noted:

(1) As noted above, the 5-SASL probe provides an approximate model for z-axial motion, but due to "wobble" of the nitroxide ring with respect to the long axis of the stearic acid chain, some limited amplitude z-axis averaging also occurs (Griffith & Jost, 1976). The departure from pure axial motion is greatest at the higher temperatures. A comparison of the 5-SASL V_1 spectrum at 30 °C (Figure 2) with spectra calculated by Griffith & Jost (1976) indicates that the wobble amplitude of the nitroxide axis with respect to the normal to the bilayer is on the order of 30°. This will produce limited, but significant, x–z and y–z motional averaging; thus the 5-SASL model system should probably be considered as quasi-anisotropic, producing spectral behavior which should be intermediate between that expected from isotropic diffusion and that expected from pure z-axial rotational diffusion. For pure z-axial rotational diffusion, the spectral region affected by rotational motion should include only the six x and y turning points in the center of the spectrum (at X band); the L'' and H'' regions should be nearly independent of x–y averaging. Hence, for pure z-axial motion, only the C'/C parameter should vary significantly with the rate of x–y averaging, and plots of L''/L or H''/H vs. C'/C should yield nearly horizontal curves at the rigid lattice limit values of these parameters. The observed behavior of the 5-SASL system is intermediate between that observed for isotropic motion and that expected for pure z-axial motion, further indicating that 5-SASL probably exhibits motional behavior intermediate between isotropic and pure z-axial. Thus the observed 5-SASL behavior in Figures 4 and 5 should probably be considered as lower bounds for the behavior of a pure z-axial system. The expected behaviors should be nearly flat curves at L''/L and H''/H values of about one.

(2) It must also be noted that use of the spectral parameters and plots of the type defined above will be most useful when the spectral turning points in the region of interest are essentially stationary. Nonstationary turning points undergoing averaging will vary in intensity, position, and resolution as motional rates change. The increases in the 9-GHz L''/L and H''/H ratios observed for temperatures above 15–20 °C with both of the axial motion lipid systems (Figure 4), for example, probably result from loss of intensity and resolution of the outer L and H turning points, rather than from buildup of intensity in the L'' and H'' regions. Additional discussion of this point is published elsewhere (Johnson & Hyde, 1981).

(3) The principal values of the nitroxide magnetic hyperfine and g tensor elements differ somewhat between the five-membered rings of the CSL and 5-SASL spin probes used for the axial motion models and the six-membered Mal-6 label used in the isotropic motion studies. At 35 GHz these differing values will affect the relative positions of the turning points somewhat and may affect the detailed behavior of the spectral intensity ratios. Thus, while the 35-GHz operation may yield better spectral resolution, it will also be necessary to ensure that a particular spectral ratio has the same significance for differing systems. This problem should be relatively minor for the 9-GHz operation.

(4) The results reported here should be applicable to membranes and other systems in which rotational diffusion is occurring within an anisotropic potential. Rotational diffusion of an asymmetric molecule within an isotropic medium should produce spectral behavior somewhat different from that observed here (Robinson & Dalton, 1980; Hyde & Thomas, 1980). Likewise, both of the lipid systems studied here probably exhibit either jump or free diffusion, while large molecules such as membrane proteins probably exhibit Brownian diffusion. Thus the behavior for larger molecular systems may be modified somewhat from that observed here.

The validity of comparing the ST-EPR spectral behavior for Mal-6-labeled Hb in aqueous solutions with those of spin probes in lipid bilayers might also be questioned since the nitroxide environments and diffusion characteristics differ markedly. However, Gaffney (1979) has shown that the basic ST-EPR spectral behavior of CSL undergoing isotropic rotational diffusion in diisobutyl phthalate is quite similar to that of Mal-6-labeled Hb in water–glycerol solutions. An L''/L vs. C'/C plot of the CSL–thiourea y-axial motion and of the CSL–diisobutyl phthalate isotropic motion data from Gaffney (1979) also shows behavior very similar to that which we observe in Figure 5. Furthermore, the saturation characteristics of immobilized Mal-6-labeled Hb and of CSL in deoxygenated DPPC–cholesterol lipid dispersions in the slow motion limit are quite similar (L. Fung and M. Johnson, unpublished observations). Thus the comparison would appear to be valid.

For membrane systems the presence of oxygen may also be of concern. Hyde and co-workers (Popp & Hyde, 1981; Subczynski & Hyde, 1981) have shown that Heisenberg spin exchange between paramagnetic oxygen molecules and nitroxide spin probes in lipid bilayers produces significant changes in the ST-EPR spectral behavior of those spin probes. In the present work we have removed oxygen from the bilayer systems by purging extensively with nitrogen. At 9 GHz this was accomplished through the use of a gas-permeable capillary as an EPR cell and by waiting until the ST-EPR spectra showed no further change due to diffusion of oxygen out of the system. At 35 GHz the lipid dispersions were gassed extensively with nitrogen and loaded into glass capillaries under nitrogen atmosphere, and the capillaries were then sealed. At 9 GHz the C'/C ratio appears to be particularly affected by the presence of oxygen (Popp & Hyde, 1981); thus the presence of oxygen in membrane systems may affect the apparent motional anisotropy. (Oxygen is much less soluble in aqueous solutions than in lipid bilayers and does not appear to substantially affect the ST-EPR spectra of aqueous systems at normal atmospheric concentrations.) Additional work will be required to determine the extent to which oxygen would affect the spectral parameter correlation plots described here.

In summary, the present work indicates the feasibility of characterizing anisotropic rotational diffusion within ordered environments such as those of membranes. The use of plots in which the behavior of spectral parameters from different regions of the ST-EPR spectra are correlated appears to be potentially useful in comparing different types of motion. Parameter correlation plots of L''/L and H''/H vs. C'/C of X-band spectra provide us with information on different types of motions. At X band, y-axial diffusion appears to produce a large minimum plateau in both L''/L vs. C'/C and H''/H vs. C'/C plots, while isotropic motion produces H''/H or L'/L values which monotonically decrease to zero as motion increases. In the same plots, quasi-anisotropic z-axial rotational diffusion produces minimum values of about 0.5 for both H''/H and L''/L; pure z-axial rotation would be expected to produce nearly flat curves at L''/L and H''/H values of about 1.0. At Q band, y-axial motion is readily distinguishable from isotropic motion in both the B'/B vs. C'/C plot and D'/D vs. C'/C plot (Figure 8). The 5-SASL system shows behavior close to that for isotropic motion; pure z-axial motion would be expected to show somewhat "flatter" behavior in the D'/D vs. C'/C plot. Comparison of the ST-EPR behaviors at 9 and 35 GHz provides additional resolution of the motional behavior.

Acknowledgments

We thank Dr. James S. Hyde for providing access to the Q-band EPR equipment and Dr. Chris Felix for assistance with the equipment at the National Biomedical ESR Center. The assistance of Robert Ziaja and Eugene Snowden of Wayne State University in spectral parameter measurement and in construction of the TPX capillaries is also greatly appreciated.

References

Baroin, A., Bienvenue, A., & Devaux, P. F. (1979) *Biochemistry 18*, 1151–1155.

Beth, A. H., Venkataramu, S. D., Balasubramian, K., Dalton, L. R., Robinson, B. H., Pearson, D. E., Park, C. R., & Park, J. H. (1981) *Proc. Natl. Acad. Sci. U.S.A. 78*, 967–971.

Davoust, J., Bienvenue, A., Fellman, P., & Devaux, P. F. (1980) *Biochim. Biophys. Acta 596*, 28–42.

Delmelle, M., Butler, K. W., & Smith, I. C. P. (1980) *Biochemistry 19*, 698–704.

Favre, E., Baroin, A., Bienvenue, A., & Devaux, P. F. (1979) *Biochemistry 18*, 1156–1162.

Fung, L. W.-M. (1981) *Biophys. J. 33*, 253–262.

Fung, L. W.-M., SooHoo, M. J., & Meena, W. A. (1979) *FEBS Lett. 105*, 379–383.

Gaffney, B. J. (1979) *J. Phys. Chem. 83*, 3345–3349.

Gaffney, B. J., Elbrecht, C. H., & Scibilia, J. P. A. (1981) *J. Magn. Reson. 44*, 436–446.

Griffith, O. H., & Jost, P. (1976) in *Spin Labeling: Theory and Applications* (Berliner, L. J., Ed.) Vol. 1, pp 453–523, Academic Press, New York.

Hidalgo, C., Thomas, D. D., & Ikemoto, N. (1978) *J. Biol. Chem. 253*, 6879–6887.

Hyde, J. S. (1978) *Methods Enzymol. 49*, 480–511.

Hyde, J. S., & Dalton, L. R. (1979) in *Spin Labeling: Theory and Applications* (Berliner, L. J., Ed.) Vol. 2, pp 1–70, Academic Press, New York.

Hyde, J. S., & Thomas, D. D. (1980) *Annu. Rev. Phys. Chem. 31*, 293–317.

Johnson, M. E. (1978) *Biochemistry 17*, 1223–1228.

Johnson, M. E. (1979) *Biochemistry 18*, 378–384.

Johnson, M. E. (1981) *Biochemistry 20*, 3319–3328.

Johnson, M. E., & Hyde, J. S. (1981) *Biochemistry 20*, 2875–2880.

Johnson, M. E., Simon, S., Kauffman, J. W., & MacDonald, R. C. (1973) *Biochim. Biophys. Acta 291*, 587–591.

Johnson, M. E., Thiyagarajan, P., Bates, B., & Currie, B. L. (1982) *Biophys. J. 37*, 553–557.

Kirino, Y., Ohkuma, T., & Shimizu, H. (1978) *J. Biochem. (Tokyo) 84*, 111–115.

Kusumi, A., Ohnishi, S., Ito, T., & Yoshizawa, T. (1978) *Biochim. Biophys. Acta 507*, 539–543.

Kusumi, A., Sakaki, T., Yoshizawa, T., & Ohnishi, S. (1980) *J. Biochem. (Tokyo) 88*, 1103–1111.

Lemaigre-Dubreuil, Y., Henry, Y., & Cassoly, R. (1980) *FEBS Lett. 113*, 231–234.

Lentz, B. R., Barrow, D. A., & Hoechli, M. (1980) *Biochemistry 19*, 1943–1954.

Marsh, D. (1980) *Biochemistry 19*, 1632–1637.

Marsh, D., & Watts, A. (1980) *Biochem. Biophys. Res. Commun. 94*, 130–137.

Polnaszek, C. F., Marsh, D., & Smith, I. C. P. (1981) *J. Magn. Reson. 43*, 54–64.

Popp, C., & Hyde, J. S. (1981) *J. Magn. Reson. 43*, 249–258.

Recktenwald, D. J., & McConnell, H. M. (1981) *Biochemistry 20*, 4505–4510.

Robinson, B. H., & Dalton, L. R. (1980) *J. Chem. Phys. 72*, 1312–1324.

Subczynski, W. K., & Hyde, J. S. (1981) *Biochim. Biophys. Acta 643*, 283–291.
Swanson, M. S., Quintanilha, A. T., & Thomas, D. D. (1980) *J. Biol. Chem. 255*, 7494–7502.
Swift, L. L., Atkinson, J. B., Perkins, R. C., Dalton, L. R., & LeQuire, V. S. (1980) *J. Membr. Biol. 52*, 165–172.
Thomas, D. D., & Hidalgo, C. (1978) *Proc. Natl. Acad. Sci. U.S.A. 75*, 5488–5492.
Thomas, D. D., Dalton, L. R., & Hyde, J. S. (1976) *J. Chem. Phys. 65*, 3006–3024.
Watts, A., & Marsh, D. (1981) *Biochim. Biophys. Acta 642*, 231–241.

Proton Stoichiometry of Adenosine 5′-Triphosphate Synthesis in Rat Liver Mitochondria Studied by Phosphorus-31 Nuclear Magnetic Resonance†

Seiji Ogawa* and Tso-Ming Lee

ABSTRACT: The internal phosphorylation potential and the electrochemical potential for proton of respiring mitochondria at state 4 were measured simultaneously by using ^{31}P nuclear magnetic resonance and a K^+ distribution method with a K^+-specific electrode in the presence of valinomycin. From these measurements the apparent number for the proton stoichiometry for the synthesis of one ATP was estimated to be 2.2–2.4 for the scheme of the simple chemisomotic theory. It was not an integer number and showed some dependence on the metabolic conditions of mitochondria at steady states of no net phosphorylation.

According to the chemiosmotic theory of Mitchell (1966), the ATP synthesis by the ATPase inside mitochondria should be related to the electrochemical potential for proton ($\Delta\mu_H$),[1] generated across the mitochondrial membrane by respiration, in the chemical reaction

$$P_i + ADP + nH^+_{ext} \rightleftarrows ATP + nH^+_{int}$$

The free energy change, ΔG, for the ATP synthesis by this reaction is given by

$$\Delta G = \Delta G_p + n\Delta\mu_H \quad (1)$$

where

$$\Delta G_p = \Delta G_p^0 + (RT/F) \log [ATP]/([P_i][ADP])$$

and

$$\Delta\mu_H = \Delta\psi - (RT/F)\Delta pH$$

In the above equations, $\Delta\psi$ is the cross membrane electrical potential, which is negative in the internally negative case of mitochondria, and ΔG_p^0 is the standard free energy of ADP phosphorylation.

The parameter n is the stoichiometric number of protons pumped inward by the ATPase for synthesis of one ATP. In the simple chemiosmotic theory the value of n is expected to be a unique number, and for a molecular process it is likely to be an integer. Various measurements have been made to determine the value of n in mitochondria. Reported values range from 2 to 3 (Alexandre et al., 1978; Wiechmann et al., 1975; Azzone et al., 1978; Nicholls, 1974). These values were derived from measurements of the initial rates of phosphorylation and proton ejection after an oxygen pulse (Alexandre et al., 1978) or from measurements of ΔG_p and $\Delta\mu_H$ at energetically steady state, assuming the ATPase reaction is in equilibrium ($\Delta G = 0$) (Azzone et al., 1978; VanDam et al., 1980). In most of these studies the state of the external phosphorylation in the medium was monitored and the internal phosphorylation potential was estimated indirectly.

By the use of ^{31}P NMR, one can determine the internal phosphorylation potential of mitochondria directly (Ogawa et al., 1978; Shen et al., 1980) at energetically steady state. Therefore the complication due to ATP/ADP exchange transport or P_i transport can be avoided. ^{31}P NMR can also determine ΔpH at the same time, but $\Delta\psi$ has to be measured by other methods. In the present study the potassium ion distribution across the membrane in the presence of valinomycin has been measured to estimate $\Delta\psi$ (Rottenberg, 1979a). The external K^+ concentration can be monitored during NMR measurements by a K^+-specific electrode. This study is similar to our previous study where a lipophilic cation was used to estimate $\Delta\psi$ (Shen et al., 1980). In that study there was an extensive internal binding of the cation that required a large correction in estimating $\Delta\psi$. The potassium distribution should be more reliable for $\Delta\psi$ estimation because of the high concentration of K^+ inside mitochondria, so that any binding effect should be a small factor.

In the present study we have closely examined ^{31}P NMR spectra of respiring mitochondria in the presence of valinomycin in order to characterize the resonances of the internal phosphate compounds and to differentiate them from those of the external compounds. At state 4, energetical parameters in eq 1 have been measured to estimate the value of n. The apparent value of n ($n_a = \Delta G_p/-\Delta\mu_H$) is found to be 2.2–2.4

† From Bell Laboratories, Murray Hill, New Jersey 07974. *Received December 15, 1981.*

[1] Abbreviations: $\Delta\mu_H$, electrochemical potential for proton across the mitochondrial membrane; $\Delta\psi$, cross membrane electrical potential; ΔG_p^0, standard free energy of ADP phosphorylation; ΔG_p, phosphorylation potential including ΔG_p^0; P_i, inorganic phosphate; $[P_i^{int}]$, internal concentration of P_i; NMR, nuclear magnetic resonance; ppm, parts per million for NMR peak positions; rf pulses, radio-frequency pulses for nuclear spin excitation; FCCP, carbonyl cyanide *p*-(trifluoromethoxy)-phenylhydrazone; DNP, 2,4-dinitrophenol; Tris, tris(hydroxymethyl)-aminomethane; EDTA, ethylenediaminetetraacetic acid; NAD, nicotinamide adenine dinucleotide.

0006-2960/82/0421-4467$01.25/0